

Nonlinear Signal Transfer from Mouse Rods to Bipolar Cells and Implications for Visual Sensitivity

Greg D. Field and Fred Rieke¹
Department of Physiology and Biophysics
University of Washington
Box 357290
Seattle, Washington 98195

Summary

We investigated the impact of rod-bipolar signal transfer on visual sensitivity. Two observations indicate that rod-rod bipolar signal transfer is nonlinear. First, responses of rods increased linearly with flash strength, while those of rod bipolars increased supralinearly. Second, fluctuations in the responses of rod bipolars were larger than expected from linear summation of the rod inputs. Rod-OFF bipolar signal transfer did not share this strong nonlinearity. Surprisingly, nonlinear rod-rod bipolar signal transfer eliminated many of the rod's single-photon responses. The impact on sensitivity, however, was more than compensated for by rejection of noise from rods that did not absorb photons. As a consequence, rod bipolars provide a near-optimal readout of rod signals at light levels near visual threshold.

Introduction

Mammalian rod photoreceptors are highly efficient light detectors: they readily absorb incident photons, generate large single-photon responses, and maintain low noise in darkness. Behavioral sensitivity to dim light approaches limits set by noise in the rods (reviewed by Rieke and Baylor, 1998). To reach this limit, the retinal readout of the rod signals must efficiently separate the rod's light responses from the noise background in which they occur. Bipolar cells face the challenge of combining signals from multiple rods; at low-light levels, a small fraction of the rods carry visual information, while all of the rods generate noise. Many other neural circuits face similar problems of identifying a sparse signal among a population of converging, noisy inputs. Rod-bipolar signal transfer provides an excellent opportunity to investigate how neural systems resolve this problem because the signal and noise of rod responses can be accurately measured, and the importance for visual function is clear.

On a moonless night, vision relies on a flux of photons at the retina producing less than 1 photon absorption per 10,000 rods within the 0.2 s integration time of the rod signals (reviewed by Walraven et al., 1990). This low-photon flux means that at any instant, a small fraction of the rods contribute to forming the visual image. All of the rods, however, generate noise, and this noise threatens to overwhelm signals in the rods absorbing

photons. Two components dominate a rod's dark noise: continuous fluctuations due to spontaneous phosphodiesterase (PDE) activation (Baylor et al., 1980; Rieke and Baylor, 1996b) and spontaneous photon-like events due to thermal isomerization of rhodopsin (Baylor et al., 1980). The photon-like noise events have both an amplitude and time course indistinguishable from the rod's single-photon response, making them impossible to identify and eliminate. The continuous fluctuations are smaller and faster than the single-photon response. Thus, in principle, continuous noise can be attenuated by downstream processing.

Rod signals traverse the mammalian retina through a specialized pathway (Dacheux and Raviola, 1986; Smith et al., 1986): rods → rod bipolars → All (rod) amacrine cells → cone bipolars → ganglion cells. The rod bipolars are all ON cells (i.e., they depolarize to an increase in light level). Rod signals can also reach cone bipolars via gap junctions coupling rods and cones and the cone-cone bipolar synapse (Schneeweis and Schnapf, 1995; DeVries and Baylor, 1995). A third pathway has been suggested in rodent retina: physiological (Soucy et al., 1998) and anatomical (Hack et al., 1999; Tsukamoto et al., 2001) data suggest that some OFF bipolar cells receive direct input from rods. It is widely believed that the All pathway has the highest sensitivity, although there are few direct comparisons of the sensitivities of different bipolar types.

Mammalian rod bipolar cells receive input from tens to hundreds of rods, and their sensitivity depends strongly on how these inputs are combined. If the bipolar combines rod responses linearly, continuous noise generated by all of the rods will overwhelm the signal generated by the few rods receiving photons. Thus, to reach the limit of sensitivity set by the rod signals, the rod-bipolar synapse must preferentially transmit single-photon responses and suppress continuous noise (Baylor et al., 1984). This separation of signal and noise could be achieved by thresholding the rod signals (e.g., by a nonlinear dependence of synaptic gain on rod voltage) (van Rossum and Smith, 1998). Despite the attractiveness of this idea, there is no direct experimental evidence either for or against it.

To investigate the properties of rod-bipolar signal transfer, we compared light responses in mouse rods, rod bipolar, and OFF bipolar cells. Light responses of rod bipolars increased supralinearly with flash strength, while those of rods and OFF bipolars increased linearly. This indicates that rod-rod bipolar signal transfer is nonlinear. This nonlinearity preferentially transmitted large single-photon responses or responses to multiple photons while attenuating or eliminating small single-photon responses and continuous noise. Models of rod-bipolar signal transfer indicate that elimination of single-photon responses is more than compensated for by rejection of continuous noise. Thus, the nonlinearity is well positioned to provide high sensitivity at light levels near absolute threshold.

¹ Correspondence: rieke@u.washington.edu

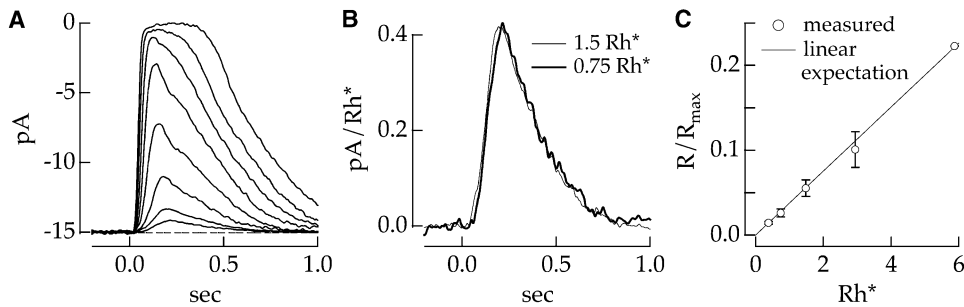


Figure 1. Linearity of Mouse Rod Light Responses

(A) Flash family is plotted for a mouse rod. Each trace is the average of 10–200 responses. The smallest response was to a flash producing on average 0.75 Rh^* , and each successive flash was twice as bright. Flashes were delivered at time 0 and were 10 ms in duration.

(B) Amplitude and kinetics of dim flash responses scale linearly with flash strength. After scaling by the flash strength, responses to dim flashes superimpose as expected for a linear process.

(C) Responses to 0–6 Rh^* scale linearly with flash strength. Each point plots the mean \pm SEM from seven rods. The straight line is the best-fit line running through the origin; it represents the expectation for a linear scaling of the rod responses with flash strength. Bandwidth: 0–20 Hz.

Results

Experimental Evidence for Nonlinear Rod-Rod Bipolar Signal Transfer

Mouse Rods Respond Linearly to Dim Flashes

Bipolar light responses reflect properties of both the rods and rod-bipolar signal transfer. Thus, we began by characterizing light responses of mouse rods. Rod responses depended linearly on flash strength for flashes producing fewer than 5–6 photoisomerizations Rh^* , as expected from previous work (Baylor et al., 1984; Nakatani et al., 1991). Figure 1A shows a family of average flash responses from a mouse rod. Figure 1B superimposes average responses to the two dimmest flashes, each scaled by the flash strength. The amplitude and time course of the responses are nearly identical, indicating that the responses scaled linearly with flash strength. Figure 1C collects measurements of the dependence of the response amplitude on flash strength from seven rods. The points cluster near the best-fit line, indicating a linear or near-linear dependence of response amplitude on flash strength.

Noise Obscures Single-Photon Responses in Mouse Rods

Identification of single-photon responses in the rod signals is limited by noise generated in the transduction cascade. The magnitude of this noise relative to the single-photon response determines how the bipolars should read out the rod responses to maximize visual sensitivity.

We characterized the rod signal and noise by examining responses to repeated presentations of a fixed-strength flash, as in Figure 2A. Baseline current fluctuations limit identification of trials in which the cell responded to the flash. This baseline noise was dominated by cellular, rather than instrumental, sources. Instrumental noise was isolated by exposing the cell to a bright, saturating light that eliminated the outer segment current. Figure 2B compares power spectra of the total noise measured both in darkness and saturating light. Exposure to saturating light decreased the magnitude of the current fluctuations for temporal frequencies below 5 Hz. Because the single-photon response is domi-

nated by similar temporal frequencies, cellular noise limits the ability to identify single-photon responses from records like that in Figure 2A. We restricted our analyses to recordings that were similarly limited by cellular noise.

The rod's dark noise and single-photon responses were characterized by constructing histograms of the response amplitudes, as in Figure 2C. The peak in the histogram near 0 pA corresponds to trials in which no photons were effectively absorbed ("failures"), and the peak near 1 pA corresponds to responses to single photoisomerizations ("singles"). The considerable overlap of the two peaks indicates that singles could not always be distinguished from failures. Thus, separation of signal and noise in the rod responses involves a tradeoff between missing small single-photon responses and rejecting noise; we explore this tradeoff in rod-bipolar signal transfer below.

We summarized the signal and noise properties of the rods by estimating the standard deviation of the dark noise relative to the mean amplitude of the single-photon response, σ_D/\bar{A} , and the standard deviation of the single-photon response relative to its mean amplitude, σ_A/\bar{A} . These ratios were estimated by fitting the amplitude histograms according to Equation 3 (smooth curve in Figure 2C; see Experimental Procedures for details). In this cell, $\sigma_D/\bar{A} = 0.28$ and $\sigma_A/\bar{A} = 0.35$. In seven cells, $\sigma_D/\bar{A} = 0.27 \pm 0.02$ (mean \pm SEM) and $\sigma_A/\bar{A} = 0.33 \pm 0.05$. In all cells, the singles and failures peaks in the histograms showed overlap like that in Figure 2C; thus, the ambiguity between noise and single-photon responses was a general property of mouse rods. For comparison, the relative amplitude of the dark noise is somewhat smaller in guinea pig and primate rods (Baylor et al., 1984; G.F. and F.R., unpublished data). We return to the implications of this difference for rod-bipolar signal transfer in the Discussion section.

Flash Responses of Rod Bipolars, but Not OFF Bipolars, Grow Nonlinearly with Flash Strength

The first indication that rod-rod bipolar signal transfer was nonlinear came from comparing the dependence of the response amplitude on flash strength in rods and rod bipolar cells. Unlike those of rods, responses of rod

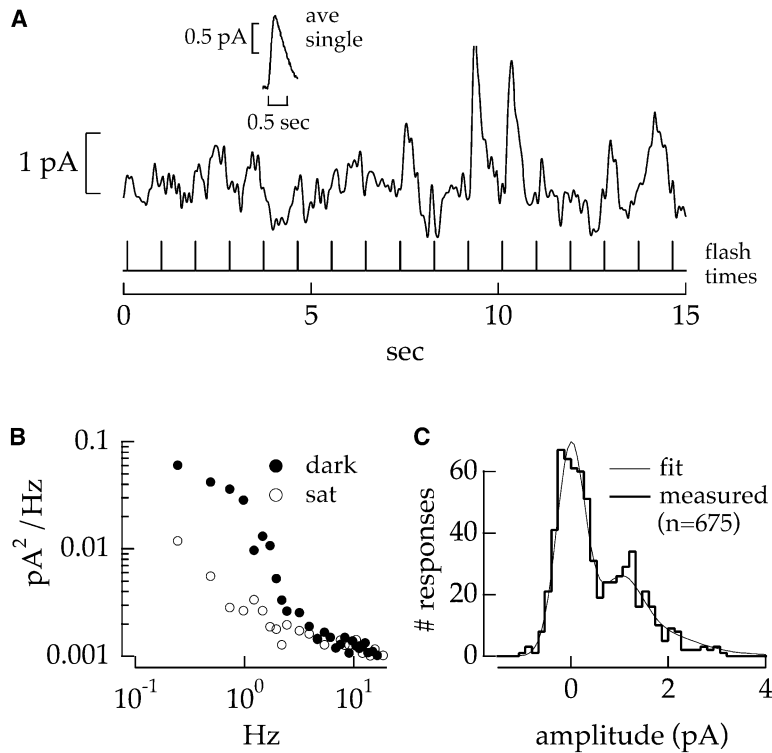


Figure 2. Single-Photon Responses and Noise in Rod Outer Segment Currents

(A) Individual responses to repetitions of a fixed-strength flash producing on average 0.6 Rh* are shown. The cell's estimated single-photon response is shown in the inset with the same amplitude and time scaling as the continuous record. Bandwidth: 0–5 Hz.

(B) Cellular noise dominates the power spectrum of noise in the outer segment current. Instrumental noise was isolated by exposing the rod to saturating light that eliminated the outer segment current. The additional noise in darkness is due to cellular noise.

(C) Distributions of dark noise and single-photon responses overlap. The amplitude of each response to a repeated flash was determined by correlating the response with a scaled version of the average response. This procedure rejects noise except that with temporal characteristics like the single-photon response. The fit to the experimental histogram was calculated according to Equation 3 with $\bar{A} = 1.03$ pA, $\bar{n} = 0.58$, $\sigma_A = 0.36$ pA, and $\sigma_D = 0.29$ pA. This procedure estimated the overlap between the dark noise and single-photon response. Dark current: 16 pA.

bipolars increased supralinearly with increasing flash strength. This supralinear dependence was absent in OFF bipolar cells.

Figure 3A shows a family of average flash responses measured from a voltage-clamped rod bipolar. The dimmest flash produced a response with a peak amplitude <1 pA, while the response to a flash twice as bright had a peak amplitude >5 pA. Figure 3B superimposes responses to two dim flashes, each divided by the respective flash strength. The current change produced by the brighter flash was larger and had faster kinetics than expected from a linear scaling of the response to the dimmer flash.

Each of the 17 rod bipolar cells analyzed showed a supralinear growth in response amplitude with flash strength like that in Figure 3B. Figure 3C plots the response amplitude against flash strength from these cells. The straight line runs from the origin to the point with the largest response per photoisomerization. This line has unity slope, and thus represents the expectation for a linear scaling of the bipolar response with flash strength. Responses to dim flashes fell short of this expectation. This difference is highly significant ($p < 10^{-5}$ for lower five points). Changing the response per photoisomerization would shift the line vertically without changing its slope in this log-log plot; no such vertical shift provides an adequate fit to the measurements. Each individual rod bipolar showed a similar nonlinear intensity-response relation. The linear behavior of the rods (Figure 1C) and the supralinear behavior of the rod bipolars is consistent with a nonlinearity in signal transfer that attenuates small rod responses while maintaining large ones.

The nonlinearity in the light responses of rod bipolars

was not due to amacrine feedback to the bipolar axon terminal or the activity of voltage-activated conductances in the soma or axon terminal. We inhibited amacrine feedback with 100 μM picrotoxin and 5 μM strychnine. As above, we recorded from bipolar cells under voltage clamp. Under these conditions, the voltage in the soma and axon terminal should have remained constant. The supralinear increase in response amplitude with flash strength remained under these conditions (eight rod bipolars; data not shown), indicating that the nonlinearity was generated at the rod-bipolar synapse or by events in the bipolar dendrites. When the bipolar voltage is not clamped, events in the soma and axon terminal could shape the bipolar responses. However, these events are unlikely to undo a nonlinearity already present in the input currents to the cell, particularly when the nonlinearity effectively eliminates the bipolar response (e.g., smallest response in Figure 3A).

Light responses of OFF bipolars depended linearly on flash strength. Figure 3D shows a family of responses from an OFF bipolar to the same flash series as the rod bipolar in Figure 3A. Figure 3E superimposes scaled responses to flashes with strengths identical to those for the rod bipolar in Figure 3B. Responses in the OFF bipolar scaled nearly linearly with flash strength, even for the smallest measurable responses. A similar dependence of response amplitude on flash strength was observed in each of eight OFF bipolar cells. Figure 3F collects measurements from these cells, analyzed identically to the rod bipolars in Figure 3C. The measured points fall close to the line of unity slope, showing the expectation if the response amplitude scaled linearly with flash strength. Differences between measured and expected points were not significant ($p > 0.1$ for lower

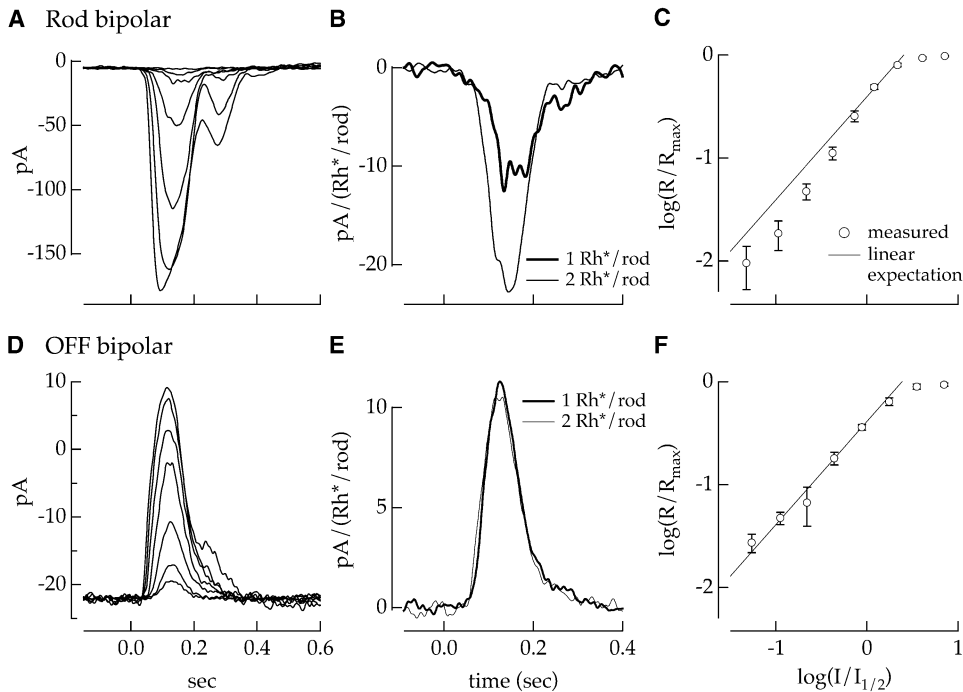


Figure 3. Dependence of Bipolar Responses on Flash Strength

(A) Flash family is plotted for a voltage-clamped rod bipolar cell. Each trace is the average of 5–20 responses. The smallest response is to a flash producing 0.25 Rh*/rod, and each successive flash was twice as bright. Flashes were delivered at time 0 and were 10 ms in duration. Holding potential: –60 mV.

(B) Rod bipolar responses depended supralinearly on flash strength. Responses to two dim flashes were divided by the flash strength and superimposed. The response to the brighter flash was larger and faster than expected from a linear scaling of the response to the dimmer flash.

(C) Dependence of response amplitude on flash strength is shown for 17 rod bipolars. Response amplitudes for each cell were normalized by the maximum response and flash strengths were normalized by that producing a half-maximal response. Maximal responses averaged 65 ± 40 pA (mean \pm SD), and half-maximal flash strengths averaged at 2.8 ± 1.5 Rh*/rod. Responses were averaged across a 2-fold range of normalized flash strengths. Each point represents the mean \pm SEM from 17 cells.

(D) Flash family is plotted for a voltage-clamped OFF bipolar. Flash strengths and recording conditions were the same as those for the rod bipolar in (A).

(E) OFF bipolar responses depended linearly on flash strength. Responses to dim flashes superimposed when scaled by the flash strength.

(F) Dependence of response amplitude on flash strength is shown for eight OFF bipolars. Measured response amplitudes from these cells have been collected and analyzed as in (C). Maximal responses averaged 35 ± 16 pA (mean \pm SD) and half-maximal flash strengths averaged 2.1 ± 1.1 Rh*/rod. Bandwidth: 0–30 Hz.

five points). Thus, rod-OFF bipolar signal transfer does not exhibit the strong nonlinearity of rod-rod bipolar signal transfer.

Flash Responses of Rod Bipolars, but Not OFF Bipolars, Show Large Trial-to-Trial Fluctuations

A second indication that rod-rod bipolar signal transfer was nonlinear came from measuring fluctuations in the responses to repeated presentations of a fixed-strength flash. Fluctuations in the responses of rod photoreceptors follow expectations from the Poisson statistics that govern photon absorption. If the rod bipolars linearly summed their rod inputs, fluctuations in their responses would also follow Poisson statistics. Instead, fluctuations in the rod bipolar responses were much larger.

Figure 4A shows eight individual responses of a voltage-clamped rod bipolar to a flash producing on average 0.6 Rh*/rod. On several trials, the cell failed to respond, while in others, the response was clear. The identification of responses and failures was much less ambiguous in rod bipolar cells than in the rods (compare Figures 2A and 4A, which are measured at identical flash

strengths). This difference was confirmed by constructing histograms of the response amplitudes in four rod bipolars, two of which are shown in Figure 4C. The histograms show several distinct peaks, corresponding to trials in which the cell failed to respond (failures) and those in which the response was clear. The peaks corresponding to failures and responses overlapped much less than those for the rod responses (Figure 2C). Thus, rod-rod bipolar signal transfer discretizes the rod responses, separating them into clearly defined categories. This discretization cannot be explained by a linear summation of the rod signals; linear summation would average across the distribution of rod responses and create a smaller, rather than larger, separation between responses and failures. The discretization can be explained by a nonlinearity in signal transfer that transmits large single-photon responses and attenuates noise and small single-photon responses.

The high probability of failures in Figure 4A provided additional evidence that many single-photon responses in the rods were eliminated in rod-rod bipolar signal

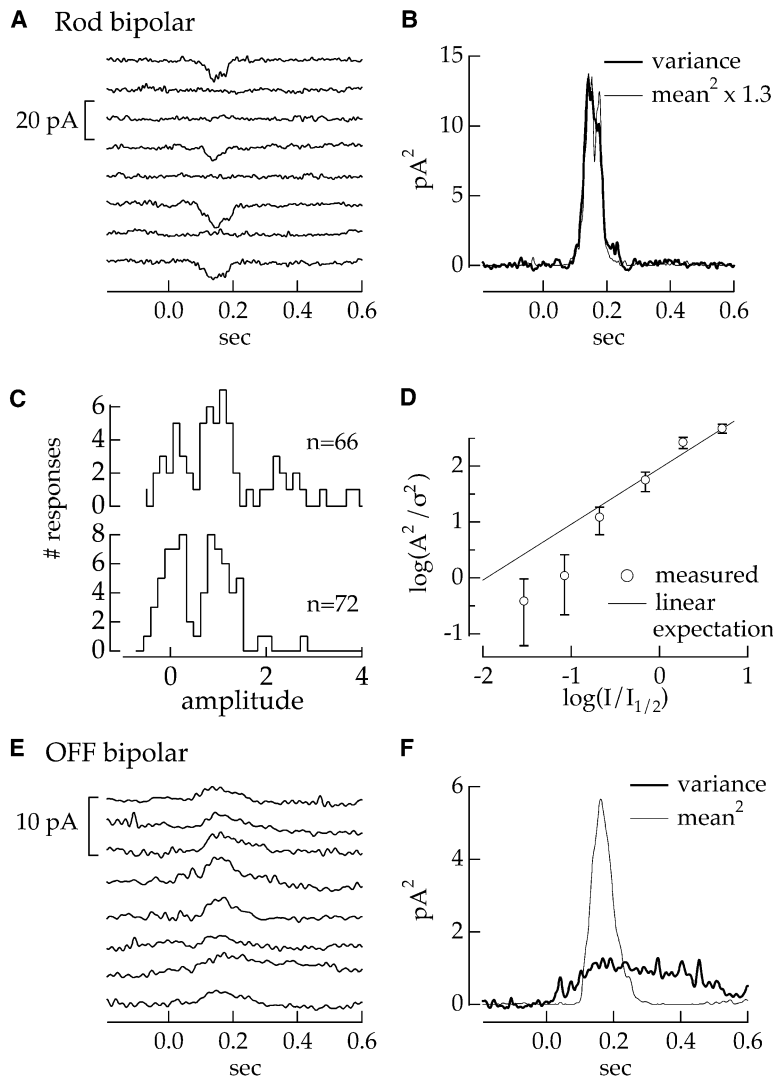


Figure 4. Rod Bipolar, but Not OFF Bipolar, Generated Discrete Responses to a Repeated Fixed-Strength Flash

(A) Individual responses are plotted from a rod bipolar to a flash producing on average 0.6 Rh^{*}/rod. Flashes were delivered at time 0 and were 10 ms in duration. Holding potential: -60 mV; mean current at this potential: -5 pA.

(B) Variance and square of the mean response are compared for a series of 20 trials, including those in (A). The variance in darkness has been subtracted to isolate the variance increase produced by the flash. The square of the mean response has been scaled to fit the variance.

(C) Histograms show response amplitudes for two rod bipolars to repetitions of a dim flash producing on average 0.25 Rh^{*}/rod. Amplitudes were estimated by correlating each response with a scaled version of the average response and normalizing so that the first nonzero peak in the histogram is centered on an amplitude of one.

(D) Ratio of the mean squared response to the variance (as in [B]) is plotted as a function of flash strength. Flash strengths in each cell have been normalized by that producing a half-maximal response. The results are plotted as mean ± SEM for 12 rod bipolars. The straight line represents the variance expected from Poisson fluctuations in photon absorption and a convergence of 20 rods onto the bipolar.

(E) Individual responses are plotted from an OFF bipolar to eight presentations of a flash producing on average 0.6 Rh^{*}/rod. Holding potential: -60 mV; holding current at this potential: -12 pA.

(F) Variance and square of the mean response are compared for a series of 20 trials, including those in (E). Bandwidth: 0–30 Hz.

transfer. Failures occurred in 9 of 20 trials recorded at this flash strength. This ratio of responses to failures would be expected from a Poisson distribution with a mean of less than one event per trial. This is much less than the expected number of photoisomerizations produced by this flash in the rods providing input to the rod bipolar. Mouse rod bipolar cells receive input from ~20 rods (Tsukamoto et al., 2001); at least ten of these rod inputs should be intact in the recorded bipolars (see Experimental Procedures). Thus, a flash producing an average of 0.6 Rh^{*}/rod should produce 6–12 Rh^{*} in the collection of rods providing input to the bipolar. The likelihood of this flash producing no photoisomerizations on 9 of 20 trials is 10^{-14}. Thus, the trial-to-trial fluctuations in the response are inconsistent with Poisson variability in photon absorption.

Response fluctuations were compared with expectations from Poisson statistics without explicitly identifying responses and failures by computing the variance and the square of the mean response. Figure 4B compares the light-dependent variance with the square of the mean for the same cell and flash strength as Figure 4A. The similarity in the shape of the variance and the

square of the mean indicate that the time course of the cell's response was relatively constant, while its amplitude varied from trial to trial, consistent with the qualitative impression from Figure 4A. If the response variability is caused by Poisson fluctuations in photon absorption, the ratio of the square of the mean to the variance estimates the average number of Rh^{*} in the pool of rods providing input to the bipolar cell. In this case, the ratio indicated an average of 0.7 Rh^{*} per flash. This estimate is consistent with that from counting failures in Figure 4A, but considerably less than the expectation of 6–12 Rh^{*} based on the flash strength and expected number of rods within the bipolar's receptive field (see above).

Fluctuations in the responses to a repeated flash were measured in 12 rod bipolars. Each cell showed trial-to-trial fluctuations, like those in Figures 4A and 4B. Results from these cells are collected in Figure 4D, which plots the square of the mean response divided by the light-dependent variance as a function of the flash strength. Poisson fluctuations predict a linear scaling of this ratio with flash strength, as indicated by the straight line in the figure; because this is a log-log plot the slope of

this line is fixed. The measured ratios have a steeper-than-linear dependence on flash strength. A similar non-linear dependence was observed in the individual cells. The inability to explain the measured fluctuations based on the Poisson statistics governing photon absorption is consistent with elimination of many single-photon responses due to nonlinear signal transfer from rods to rod bipolars.

OFF bipolars showed considerably smaller trial-to-trial fluctuations than rod bipolars. Figure 4E shows eight individual responses of an OFF bipolar to a flash with the same strength as that in Figure 4A. Unlike rod bipolars, the OFF bipolar responded to each presentation of the flash. Figure 4F compares the variance with the square of the mean response. The difference between the time course of the variance and the square of the mean indicates that fluctuations in the response shape, presumably due to noise occurring after rod phototransduction, contributed substantially to the variance. Nonetheless, the ratio of the square of the mean to the variance was much smaller in OFF bipolars than rod bipolars.

Implications of Nonlinear Signal Transfer for Visual Sensitivity

The experiments of Figures 1–4 indicate that signal transfer from mouse rods to rod bipolar cells is nonlinear. The properties of this nonlinearity determine which aspects of the rod responses are transmitted to the bipolar and which are suppressed. Thus, the nonlinearity has an important impact on visual sensitivity. We first modeled rod-rod bipolar signal transfer to estimate the properties of the nonlinearity. We then used the resulting model to determine the impact of the nonlinearity on the detectability of dim flashes. These calculations indicate that nonlinear signal transfer from rods to rod bipolars provides a near-optimal readout of the rod array at light levels near visual threshold.

Model for Rod-Rod Bipolar Signal Transfer

We considered models for rod-rod bipolar signal transfer in which an instantaneous nonlinearity either preceded (Figure 5D) or followed (Figure 5A) the pooling of rod responses. The aim was to determine which model could account for two aspects of the measured bipolar response: the nonlinear dependence of the mean response on flash strength (Figure 3C) and the discreteness of the bipolar responses to repeated presentations of a dim flash (Figure 4C).

Model 1: Nonlinearity after Pooling

Predicted bipolar responses were generated in three steps. (1) Rod responses were generated according to Equation 3. (2) The rod responses were summed. (3) The summed signal was passed through a time-independent nonlinearity (Figure 5A; see Experimental Procedures for details). The nonlinearity was taken to be a cumulative Gaussian. We independently varied the midpoint and standard deviation of the cumulative Gaussian in an attempt to account for the measured bipolar responses.

This model failed because matching the discreteness of the bipolar response required a nonlinearity with a small standard deviation—a threshold-like nonlinearity. However, applying such a nonlinearity to the summed rod responses caused the dimmest flashes to go unde-

tected and thus made the response amplitude overly sensitive to flash strength. Figures 5B and 5C illustrate these discrepancies.

Figure 5B compares the measured dependence of the response amplitude on flash strength with predictions for a model in which the midpoint and standard deviation of the cumulative Gaussian were equal and one where the standard deviation was 0.1 times the midpoint. The nonlinearities themselves are shown in the inset. Reasonable fits to the measured dependence of response amplitude on flash strength required that the cumulative Gaussian have a large standard deviation (i.e., that the nonlinearity increases gradually with increasing response amplitude).

Only threshold-like nonlinearities, however, captured the discrete nature of the distribution of responses to a repeated dim flash. Measured distributions show two clear peaks, corresponding to trials in which the cell failed to respond to the flash and those in which it produced a response (see Figure 4C). Figure 5C plots the predicted response distributions for a flash producing on average 0.25 Rh*/rod. The threshold-like nonlinearity produced a two-peaked distribution qualitatively similar to that measured. The gradual nonlinearity produced a response distribution with a single, broad peak substantially different than that measured.

Discrepancies between measured and predicted bipolar responses, such as those in Figures 5B and 5C, were found for all combinations of midpoints and standard deviations of the cumulative Gaussian. Thus, we did not further consider models in which pooling of rod responses preceded the nonlinearity.

Model 2: Nonlinearity Prior to Pooling

Predicted bipolar responses were generated in three steps. (1) Rod responses were generated as above. (2) Each rod response was passed through a nonlinearity. (3) The resulting signals were summed (Figure 5D; see Experimental Procedures for details). As above, the nonlinearity was taken to be a cumulative Gaussian. In this case, the midpoint and the standard deviation of the cumulative Gaussian could be adjusted to provide a reasonable description of the bipolar responses.

The measured bipolar responses provided several constraints on the form of the nonlinearity. Gradual nonlinearities failed to account for the discreteness of the bipolar response, while threshold-like nonlinearities could account for the discreteness and the dependence of response amplitude on flash strength. Unlike the first model, the strong dependence on flash strength produced by the nonlinearity was smoothed by averaging across rod signals because the nonlinearity was positioned prior to pooling. Agreement with experiment required that the nonlinearity eliminate many single-photon responses (i.e., that the midpoint of the cumulative Gaussian was large). This constraint is described in more detail below.

Figure 5E compares the predicted and measured dependence of the response amplitude on flash strength. The smooth curves plot predictions from cumulative Gaussian nonlinearities with midpoints 1.0 and 1.3 times the average amplitude of the single-photon response. The smaller midpoint predicted a more gradual increase in response amplitude than observed. The overprediction of responses to dim flashes became worse as

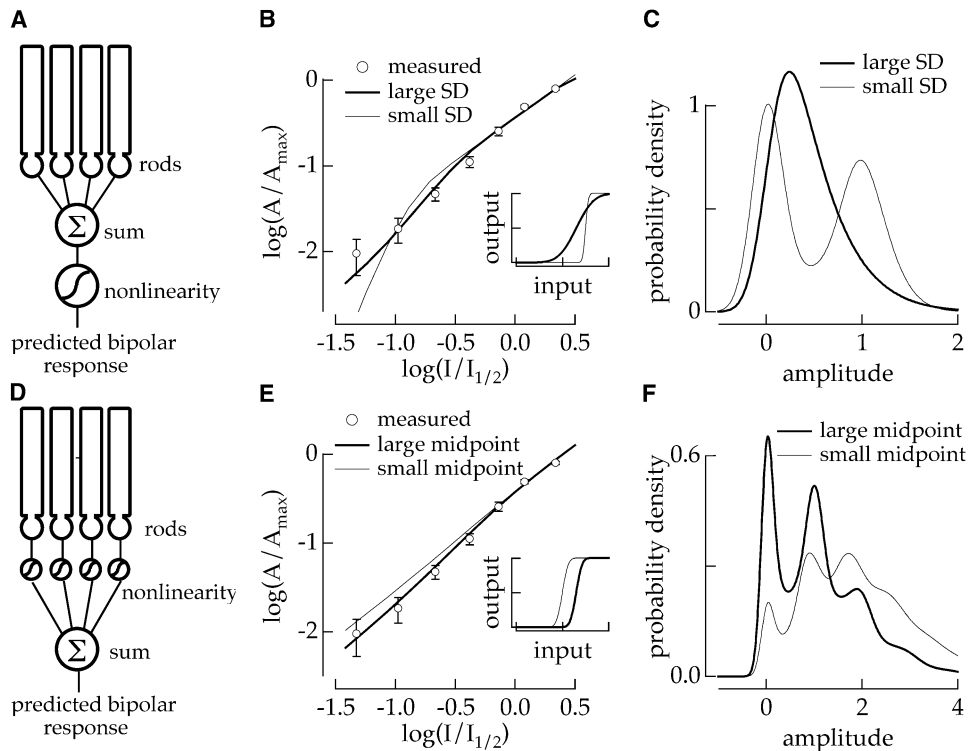


Figure 5. Models for Rod-Rod Bipolar Signal Transfer

- (A) Model 1: rod responses were linearly summed and then passed through a time-independent nonlinearity. We assumed the bipolar received input from 20 rods.
- (B) The measured dependence of response amplitude on flash strength is compared to that predicted by Model 1. Predictions are shown for two cumulative Gaussian nonlinearities, one with a standard deviation equal to the midpoint and one with a standard deviation 0.1 times the midpoint. The cumulative Gaussians are shown in the inset. Only the cumulative Gaussian with a large standard deviation provided an adequate fit to the data.
- (C) Predicted distributions of the bipolar responses to repetitions of a flash producing an average of 0.25 Rh*/rod are compared for the two nonlinearities in (B).
- (D) Model 2: rod responses were passed through a time-independent nonlinearity prior to linear summation.
- (E) The measured dependence of response amplitude on flash strength is compared to that predicted from Model 2. Predictions are shown for cumulative Gaussians with midpoints of 1 and 1.3 and a standard deviation of 0.1 (see inset). The cumulative Gaussian with the larger midpoint provided a better fit to the data.
- (F) Predicted amplitude distributions are compared, as in (C), for the two nonlinearities in (E).

the midpoint of the cumulative Gaussian was decreased and more of the rod's single photon responses were retained. A model with a midpoint of 1.2 was ten times less likely to explain the experimental measurements than one with a midpoint of 1.3. Similarly, cumulative Gaussians with a midpoint substantially larger than 1.3 predicted a dependence of response amplitude on flash strength steeper than that observed. A midpoint of 1.4 was three times less likely to explain the measurements than one of 1.3.

The cumulative Gaussian with the larger midpoint was also more consistent with the measured distribution of responses to a repeated dim flash. Figure 5F compares predicted response distributions for cumulative Gaussians with midpoints of 1.0 and 1.3 for a flash producing on average 0.25 Rh*/rod. The smaller midpoint predicts fewer small responses and more large responses than observed (see Figure 4C) because the model retains too large a fraction of the rod's single-photon responses. The distribution predicted by the cumulative Gaussian with a larger midpoint is qualitatively similar to that ob-

served. Cumulative Gaussians with standard deviations >0.2 failed to capture the discreteness of the measured responses.

The analysis of Figure 5 indicates that the measured rod bipolar responses are most consistent with a nonlinearity acting on each rod signal before these signals are combined. Only threshold-like nonlinearities provided reasonable agreement with experiment. The position of the nonlinearity relative to the single-photon response caused it to eliminate or severely attenuate many of the rod's single-photon responses. The cumulative Gaussian nonlinearity that best explains the bipolar responses—with a midpoint 1.3 times the average single-photon response—eliminates about 75% of the rod's single-photon responses.

Separation of Signal and Noise and Impact on Visual Sensitivity

Elimination of single-photon responses in rod-rod bipolar signal transfer is counterintuitive: the rod's photo-transduction machinery is well suited for the task of detecting single photons, yet the majority of these sig-

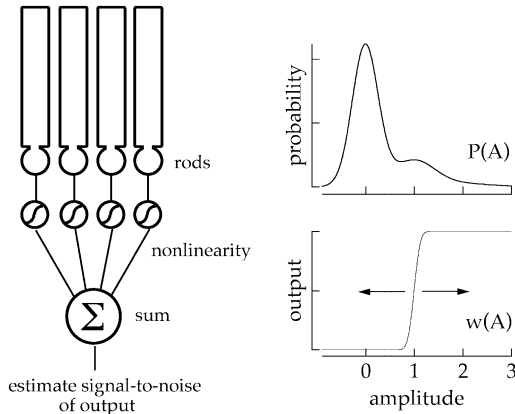


Figure 6. Procedure for Estimating the Signal-to-Noise of the Rod Array for Linear and Nonlinear Readouts

The distribution of rod signals $P(A)$ was described by Equation 3. We applied a nonlinear weighting function, $w(A)$, to this distribution and calculated the ratio of the mean squared to the variance of the weighted amplitudes. The nonlinear weighting function suppressed small responses and retained large ones. By varying the x axis position of the nonlinearity, we investigated how weighting responses, based on their amplitude, affected the signal-to-noise of the output.

nals are apparently discarded in transfer to the rod bipolar. At the same time, linear summation of the rod inputs would retain all of the rods' dark noise, compromising sensitivity at low-light levels. Because the dark noise and single-photon response distributions overlap (Figure 2C), rejection of noise will invariably lead to elimination of some single-photon responses. We explored this tradeoff by estimating the signal-to-noise ratio of the rod responses for linear and nonlinear readouts of the rod array. These calculations indicate that the nonlinearity in rod-rod bipolar signal transfer maximizes the signal-to-noise of the rod bipolar response at light levels near absolute threshold.

Figure 6 outlines our approach. For a given flash strength, we estimated the distribution of rod responses $P(A)$ from Equation 3. We applied a time-independent nonlinearity, $w(A)$, to this distribution so that each amplitude A was rescaled to $A \times w(A)$ and calculated the distribution of the rescaled amplitudes. To determine how sensitivity varied with the properties of the nonlinearity, we calculated the signal-to-noise ratio of the weighted signals (i.e., the mean squared of the rescaled amplitudes divided by their variance).

At visual threshold, photon absorptions occur at a rate of about 1 per 10,000 rods within the integration time of the rod response. We investigated the impact of nonlinear readouts of the responses of single rods on sensitivity at these light levels. The rod's integration time provides a natural time scale for this problem, as photons arriving further apart in time will generate independent responses. Thus, we considered the distribution, $P(A)$, of the rod responses to a flash producing 0.0001 Rh*, as in Figure 7A. Because the probability of photon absorption is extremely low, the noise dominates the distribution except for large response amplitudes. The signal and noise distributions cross at an amplitude 1.2 times that of the average single-photon response;

thus, responses with amplitudes <1 are most likely caused by noise, rather than photon absorption. Separating signal and noise involves eliminating these small responses while retaining those with an amplitude >1.2 (i.e., those most likely to be due to photon absorption).

A general approach to the problem of separating signal and noise is to weight each response by the probability that it is from the signal distribution. This weighting function $w_{\text{opt}}(A)$ is:

$$w_{\text{opt}}(A) = \frac{P_S(A)}{P_N(A) + P_S(A)}, \quad (1)$$

where A is the response amplitude and $P_S(A)$ and $P_N(A)$ are the probabilities of obtaining a response of amplitude A from the signal and noise distributions (e.g., Figure 7A). Figure 7B compares the nonlinear weighting function calculated according to Equation 1 with the cumulative Gaussian nonlinearity estimated from the measured bipolar responses as in Figures 5D–5F (midpoint = 1.3, standard deviation = 0.1).

The x axis position of the nonlinear weighting function in Figure 7B has an important bearing on the signal-to-noise ratio of the weighted rod signals. To investigate this dependence, we calculated the signal-to-noise ratio from the distributions in Figure 7A for a cumulative Gaussian nonlinearity, $w(A)$, whose midpoint varied. Signal-to-noise was defined as the mean squared of the weighted signals divided by their variance. Calculated signal-to-noise ratios were normalized by the signal-to-noise calculated for linear pooling, i.e., $w(A) = 1$. Figure 7C plots the normalized signal-to-noise ratio as a function of the nonlinearity midpoint for a flash producing 0.0001 Rh*. The nonlinearity with a midpoint of 1.2 produced a 420-fold increase in signal-to-noise compared to a linear combination of the rod signals. The nonlinearity estimated from the bipolar responses (midpoint = 1.3) improved the signal to noise >350 -fold. Thus, at light levels near absolute threshold, the nonlinear properties of rod-rod bipolar signal transfer provide a near-optimal readout of the rod array.

The properties of the nonlinearity that produced the highest signal-to-noise depended on the light level. Figure 7D shows the rod signal and noise distributions for a flash producing 0.01 Rh*, 100 times brighter than absolute threshold. In this case, the signal and noise distributions cross at an amplitude 0.85 times that of the mean single-photon response. Accordingly, the weighting function calculated from Equation 1 is shifted to the left of that determined from the bipolar responses (Figure 7E). The improvement in signal-to-noise (Figure 7F) peaked at a factor of eight to nine, while the nonlinearity estimated from the bipolar responses produced an improvement of a factor approximately four. Thus, at light levels significantly above absolute threshold, nonlinear signal transfer was not well matched to the rod signal and noise.

Discussion

We have investigated the properties of signal transfer from mouse rods to bipolar cells, particularly their impact on absolute visual sensitivity. Our experiments lead

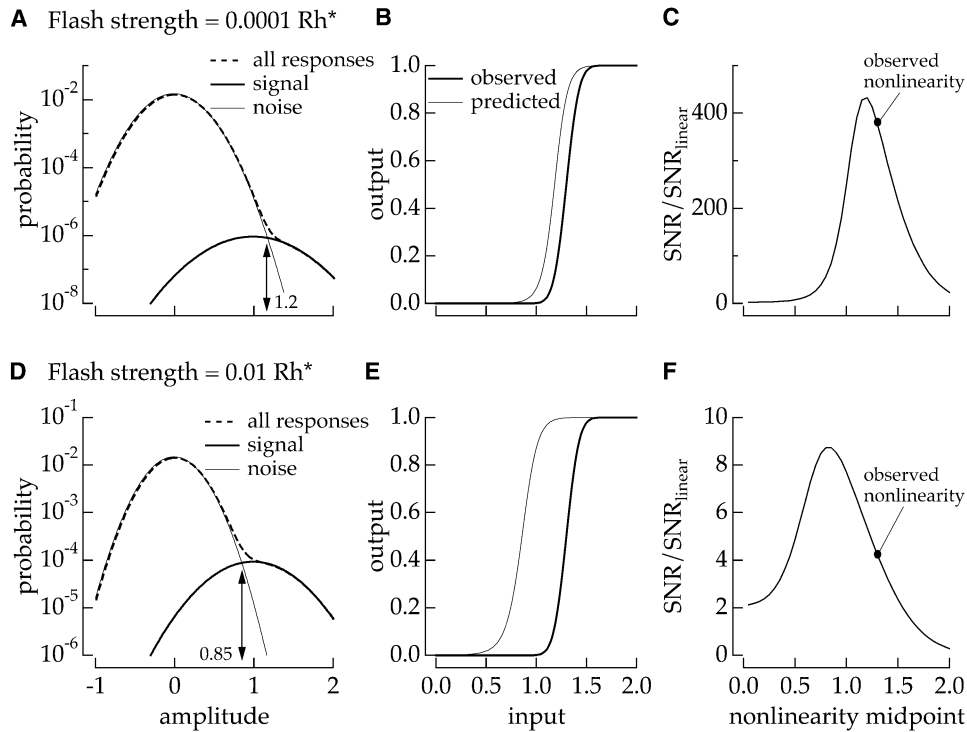


Figure 7. Implications of Nonlinear Signal Transfer for Sensitivity

(A) Distribution of rod responses calculated from Equation 3 is plotted for a flash near visual threshold. The dashed line shows the complete distribution, the thick line shows the distribution of responses to photon absorption (the signal component), and the thin line shows the distribution of responses when no photons are absorbed (the noise component).

(B) Comparison of nonlinear weighting functions $w(A)$ estimated from the bipolar responses, as in Figure 5 (thick line), or predicted from the rod responses in (A) and Equation 1 are compared.

(C) The signal-to-noise ratio is shown as a function of the midpoint of the cumulative Gaussian nonlinearity. Signal-to-noise was determined from the rod distributions in (A) as the mean response squared divided by the variance. The standard deviation of the cumulative Gaussian was fixed at 0.1, while the midpoint was varied.

(D) Distribution of rod responses for a brighter flash, as shown in (A).

(E) Predicted and estimated nonlinear weighting functions are compared, as in (B).

(F) The signal-to-noise ratio, as shown in (C).

to three main conclusions. (1) A nonlinearity in signal transfer from rods to rod bipolars eliminates many of the rod's single-photon responses. (2) This nonlinearity is absent or considerably less pronounced in rod-OFF bipolar signal transfer. (3) The elimination of many single-photon responses is compensated for by rejection of noise, causing a substantial improvement in sensitivity near absolute threshold. These conclusions are discussed in more detail below.

Mechanisms Generating Nonlinearity in Signal Transfer

The nonlinearity in rod-rod bipolar signal transfer could potentially be produced by transmitter release from the rods, the generation of a postsynaptic response in the bipolar dendrites, or events in the bipolar soma or axon terminal. As described below, the most likely mechanism is saturation of the postsynaptic machinery in the bipolar dendrites.

A nonlinear dependence of the rate of transmitter release on rod voltage could account for nonlinear signal transfer. Indeed, transmitter release from amphibian rods depends nonlinearly on the rod voltage (Witkovsky

et al., 1997); however, the shape of the nonlinearity causes release to be more sensitive to small changes in rod voltage than large ones. This is the opposite of the effect required to explain the measured bipolar responses.

Conductances in the bipolar soma or axon terminal could cause nonlinear signal transfer. The nonlinearity persisted, however, when the bipolar was voltage clamped and amacrine feedback to the bipolar axon terminal was suppressed. Axotomized rod bipolar cells in rat retina showed a similar nonlinear dependence of response amplitude on flash strength (Euler and Masland, 2000), although this nonlinearity was present at higher light levels than those used here. These observations indicate that nonlinear signal transfer is not generated by events in the bipolar soma or axon terminal.

A more likely mechanism is saturation of the postsynaptic machinery (van Rossum and Smith, 1998). Saturation could take place either at the bipolar cell glutamate receptors or in the transduction cascade coupling the receptors to channels. Such a saturation would cause all the channels in the bipolar to be closed in darkness. Small fluctuations in the rod voltage (e.g., due to continuous noise or a small single-photon response) would not

reduce the glutamate concentration in the synaptic cleft sufficiently to free the postsynaptic machinery from saturation. Hence, these small signals would go undetected by the bipolar. Larger changes in rod voltage (e.g., due to a large single-photon response) would reduce glutamate sufficiently to produce a postsynaptic response. This model has been studied in detail by van Rossum and Smith (1998).

Rod Circuitry in Mouse Retina

We found, surprisingly, that the light levels required to elicit half-maximal responses in both rod bipolars and OFF bipolars did not differ significantly. This might be expected if the signal reached the OFF bipolar via the rod bipolar and All amacrine. However, since the OFF bipolar response did not display the nonlinear dependence on flash strength of the rod bipolar response, it is not likely produced by All input. This implies that either the OFF bipolars get direct input from rods or that the signaling pathway through the cones and cone synapse operates at low-light levels. Similarly, some types of OFF ganglion cells in rabbit retina maintained their responses to dim lights when activity in rod bipolars was suppressed (DeVries and Baylor, 1995). However, the differences in rod-rod bipolar and rod-OFF bipolar signal transfer causes these two parallel readouts to have very different sensitivities. The implications of signal transfer for sensitivity are discussed below.

Nonlinearity and Relation to Visual Sensitivity

The fidelity of signals produced by the rods would be wasted if these signals were not reliably and effectively transmitted to other neurons in the retina. Several aspects of rod-bipolar signal transfer suggest that it, like the phototransduction process in the rods, is well suited for the task of providing high sensitivity at low-light levels.

Noise generated at the rod-bipolar synapse poses one threat to reliable photon detection. This noise appears to be minimized in two ways. First, a high rate of vesicle fusion in darkness keeps statistical fluctuations in transmitter release to a minimum (Rao et al., 1994; Rieke and Schwartz, 1996a). Second, transmitter release depends steeply on rod voltage (Belgum and Copenhagen, 1988; Rao-Mirotnik et al., 1995; Witkovsky et al., 1997), so small voltage changes produce large changes in release.

Separation of signal and noise in rod-bipolar signal transfer occurs through both linear and nonlinear mechanisms. In salamander and dogfish, the linear filtering properties of rod-bipolar signal transfer are matched to the temporal characteristics of the rod signal and noise (Ashmore and Falk, 1980; Bialek and Owen, 1990), causing temporal frequencies that carry the most information about the light inputs to be preferentially transmitted. Thus, signal transfer attenuates low temporal frequencies, which have intrinsically poor temporal resolution, and high temporal frequencies, which are dominated by continuous noise.

In mammalian retina, the sparseness of the signal in the rod array and the relatively large continuous noise poses a problem that cannot be solved by linear filtering: any linear combination of the rod responses at light levels where only 1 in 10,000 rods receives a photon

will necessarily cause the signal to be swamped by noise. Reaching the limits to sensitivity imposed by the rods requires separation of signal and noise before the rod responses are combined (Baylor et al., 1984; van Rossum and Smith, 1998). In principle, comparison of rod noise with behavioral sensitivity could show that such nonlinear processing takes place. However, existing behavioral measures vary too much to rule out a linear combination of rod signals (Schneeweis and Schnapf, 2000). Indirect evidence for a nonlinearity acting on the rod single-photon responses comes from electroretinograms in dark-adapted cats (Robson and Frishman, 1995) and mice (S. Saszik, L.J. Frishman, and J.G. Robson, personal communication). In these experiments, the initial rise of the rod bipolar component in response to a brief flash scaled supralinearly with flash strength for flashes producing around 1 Rh^*/rod (Figure 8 of Robson and Frishman, 1995).

Our recordings from mouse rod bipolar cells provide direct evidence for a nonlinearity in rod-rod bipolar signal transfer and allow us to estimate the properties of the nonlinearity relative to the rod's single-photon response. Surprisingly, the nonlinearity eliminated or severely attenuated many of the rod's single-photon responses. However, because of the sparseness of the signals in the rod array, rejection of continuous noise more than compensates for the missed single-photon responses. Thus, the nonlinearity in rod-rod bipolar signal transfer is well situated to maximize sensitivity at light levels near visual threshold. As light levels increase, however, the nonlinearity will limit the sensitivity of rod bipolars. Under these conditions, signals in OFF bipolars, which are more linear and hence retain most or all of the rod's single-photon responses, may be more sensitive than those in rod bipolars.

Pooling of Sparse Signals

Rod vision at low-light levels exemplifies a general problem: pooling of signals from an array of detectors in which the signal is sparsely represented. Cells throughout the nervous system receive converging inputs, and thus face a similar problem when a small number of the inputs are active. For example, single glomeruli in the olfactory bulb receive input from tens of thousands of olfactory receptors (reviewed by Hildebrand and Shepherd, 1997). Detection thresholds for odors are ~ 10 – 100 molecules (DeVries and Stuiver, 1961), corresponding to activation of $<1\%$ of the olfactory receptors projecting to a single glomerulus. The sparseness of signaling and large convergence creates a situation similar to that encountered in the rod array near visual threshold. A nonlinear strategy for combining signals from the receptors could improve sensitivity to weak odors by rejecting noise from the unactivated receptors.

Even in the retina, the sparseness of signals at or near absolute threshold is not restricted to the rod array. Since rod bipolar cells receive input from ~ 20 rods (Tsukamoto et al., 2001), at visual threshold less than 1% of the rod bipolars receives a photon within its receptive field per rod integration time. All (rod) amacrine cells receive input from about 20 rod bipolars (Sterling et al., 1988). Hence the rod bipolar-All synapse faces the same problem as the rod-bipolar synapse: light responses are

sparingly represented in the bipolars, and a linear pooling of bipolar responses threatens to overwhelm the signal with noise generated in all of the bipolars. The discreteness of the responses in the rod bipolars (Figure 4C) suggests that a second stage of nonlinear processing at the rod bipolar-All synapse could effectively reduce noise intrinsic to the bipolar cell or its synaptic output.

The appropriate nonlinear pooling strategy depends on the signal and noise properties of the input signals. Thus, a change in the relative amplitude of the rod's dark noise and single-photon response will have an important impact on the optimal strategy for separating both signal and noise and maximizing visual sensitivity. This dependence allows us to make predictions about nonlinear rod-rod bipolar signal transfer in other mammalian retinas. In primate rods, the amplitude of the continuous dark noise is a smaller fraction of the single-photon response than in mouse rods (Baylor et al., 1984). The smaller dark noise alters the tradeoff of rejecting noise and missing small single-photon responses such that a nonlinearity in rod-rod bipolar signal transfer in primate could retain more of the rod's single-photon responses while still effectively rejecting noise.

Experimental Procedures

All experiments used mice from strain C57BL/6. Mice were dark adapted overnight and retinas were isolated following procedures approved by the Administrative Panel on Laboratory Animal Care at the University of Washington (see Kim and Rieke, 2001). The dissection and subsequent procedures were carried out under infrared light (>900 nm) to keep the retina fully dark adapted. Isolated retinas were stored in a light-tight container at 37°C in bicarbonate-buffered Ames solution (Sigma, St. Louis, MO) equilibrated with 5% CO₂/95% O₂. During recording, cells or retinal slices were superfused with Ames solution warmed to 36.5–37.5°C. Bath temperature was monitored continuously with a thermistor placed within a few millimeters of the recorded cell. The volume of the recording chamber was 0.3–0.5 ml, and superfusion rate was 4–6 ml/min. The pH measured in the recording chamber was 7.35.

Measurements of Rod Photocurrents

Rod outer segment currents were recorded with suction electrodes following established methods (Baylor et al., 1979a; Rieke, 2000). In brief, a small piece of retina was shredded in a drop of Ames solution, and the resulting suspension was allowed to settle to the floor of a glass-bottomed recording chamber. A rod outer segment was drawn by suction into a borosilicate electrode cut and polished to a tip diameter of 1.4–1.6 μm. The solution filling the suction electrode was identical to the superfusion solution except that the bicarbonate buffer was replaced with 10 mM Hepes and 15 mM NaCl. Current collected by the suction electrode was amplified, low-pass filtered at 30 Hz (8 pole Bessel), and digitized at 1 kHz. Responses to saturating and half-saturating flashes were measured periodically to check for stability.

Photon densities (in photons μm⁻²) were converted to photoisomerizations (Rh*) using measured rod collecting areas. The collecting area of an individual rod was estimated from trial-to-trial variability in the responses to a fixed-strength flash, as in Equation 2. Assuming that Poisson fluctuations in photon absorption dominate variability in the cell's response, the mean number of photoisomerizations produced by the flash can be estimated by dividing the square of the mean response by the variance:

$$\bar{n} = \frac{\bar{I}^2}{\sigma_I^2}, \quad (2)$$

where \bar{I} is the average response and σ_I^2 is the variance increase produced by the flash. This procedure was repeated for 2–4 flash

strengths and the collecting area estimated as the slope of the best-fit line in a plot of \bar{n} against the photon density. The collecting area from eight rods was $0.52 \pm 0.07 \mu\text{m}^2$ (mean \pm SEM).

Measurements of Bipolar Responses

Light-evoked responses of bipolar cells were measured in a slice preparation (Werblin, 1978; Wu, 1987; Rieke, 2001). Slices 200–300 μm thick were cut on a vibrating microtome (Leica, Wetzlar, Germany) and held in place in the recording chamber with a nylon grid glued to a platinum ring. Electrical responses of bipolar cells were measured using perforated-patch recordings. Borosilicate patch pipettes were filled with an internal solution containing 125 mM K-Aspartate, 10 mM KCl, 10 mM HEPES, 5 mM NMG-HEDTA, 0.5 mM CaCl₂, 2 mM ATP, 0.2 mM GTP, 0.1 mM alexa-488 (Molecular Probes, Eugene, OR), and 0.5 mg/ml amphotericin-B; pH was adjusted to 7.2 with NMG-OH, and osmolarity was 280 mOsm. The pipette tip was filled with amphotericin-free solution. Filled pipettes had resistances of 12–14 MΩ, and the series resistance during recording was 20–50 MΩ.

Alexa was included in the pipette solution to permit a cell's morphology to be visualized under fluorescence at the end of a recording. Rod bipolar cells were identified by the position of their somata near the outer plexiform layer and the position of their axon terminals near the inner margin of the inner plexiform layer (Tsukamoto et al., 2001). OFF bipolars were distinguished based on the polarity of their responses. We did not attempt to subdivide OFF bipolars into classes, although we recorded exclusively from cells with somata close to the outer plexiform layer. Data were collected only from bipolar cells with strong rod-driven light responses (30%–50% of the recorded cells); thus, we did not characterize any bipolars receiving cone input primarily or exclusively. Bipolar cells were held at –60 mV to minimize activation of voltage-dependent conductances.

Light Stimuli

Light was delivered from a light-emitting diode (LED) with a peak output at a wavelength of 470 nm. Light from the LED was focused on the preparation to uniformly illuminate a circular area 650 μm in diameter, centered on the recorded cell. Light intensities measured at the preparation are given in the figure legends.

In the slice experiments, some light was absorbed before reaching the rods providing input to the recorded bipolar. Light stimuli were focused on the recorded cell through an 0.85 numerical aperture objective lens in place of the microscope condenser. The relatively high numerical aperture meant that the stimulating light was delivered at a wide range of angles, and thus most of the light traversed only a small fraction of the thickness of the slice. We estimated attenuation due to other rods in the slice to be 50% at most, based on the numerical aperture of the lens, the 200–300 μm thickness of the slice, and 1.2% absorption per μm for a rod outer segment.

Figure 4D provided verification of this calculation and a check that the recorded bipolar cells retained most of their rod inputs. The vertical position of the line in Figure 4D corresponds to an effective collecting area for the pool of rods converging on a bipolar cell. Comparing this effective collecting area to the measured rod collecting area of 0.5 μm² provided an estimate of the number of rod inputs to the bipolar—in this case 21. This is essentially identical to the expectation of 20 from anatomical measurements (Tsukamoto et al., 2001). Substantial absorption within the slice or disruption of rod-bipolar connections would cause the convergence estimated from Figure 4D to fall short of the anatomical estimate.

Models for Rod-Bipolar Signal Transfer

We used two nonlinear models to characterize rod-rod bipolar signal transfer. Details of these models are described below.

Characterization of Rod Inputs

We assumed that 20 rods converged on a bipolar cell, although similar results were obtained for a convergence of 5–40 rods. The rod inputs were described by the distribution of dark noise and the distribution of single-photon responses. These signal and noise distributions were characterized by fitting histograms of the response amplitudes to repetitions of a fixed dim flash (see Figure 2C). Amplitudes were measured by correlating each response with

a scaled version of the average response. Fits assumed that the number of absorbed photons obeyed Poisson statistics and that dark noise and variability in the single-photon response were independent and additive. In this case the probability $P(A)$ of a response with an amplitude between $A - \Delta A/2$ and $A + \Delta A/2$ is (Baylor et al., 1979b)

$$P(A) = \Delta A \sum_{n=0}^{\infty} \frac{\exp(-\bar{n})\bar{n}^n}{n!} [2\pi(\sigma_D^2 + n\sigma_A^2)]^{-1/2} \exp - \frac{(A - n\bar{A})^2}{2(\sigma_D^2 + n\sigma_A^2)} \quad (3)$$

Here, \bar{A} is the mean single-photon response amplitude and σ_A is its standard deviation, n is the number of photoisomerizations produced by the flash and \bar{n} is its mean, and σ_D is the standard deviation of the current fluctuations in darkness. To provide accurate estimates of the fit parameters, we simultaneously fit histograms measured for 2–4 flash strengths to find a common \bar{A} , σ_D , and σ_A ; \bar{n} was determined from the cell's collecting area and the flash strength. The rod inputs to each model were described by Equation 3 with $\sigma_D = 0.27$ and $\sigma_A = 0.33$ and $\bar{A} = 1.0$.

This procedure makes two assumptions about the equivalence of the signals in the outer segment and in the synaptic terminal. First, estimating the response amplitudes by correlation with a template is equivalent to applying a temporal filter matched to the rod's signal and noise. Thus, our analysis assumes that such a filter occurs prior to the nonlinearity in signal transfer (e.g., in the rod synaptic terminal). Second, we equate the distribution of responses at the rod synaptic terminal with that measured in the rod outer segment. Recent anatomical measurements show gap junctions between mouse rods (Tsukamoto et al., 2001), which could spread electrical signals among adjacent rods. It is unclear, however, if these gap junctions are operational. Furthermore, the anatomical measurements suggest that the coupling is weak, compared to amphibian retinæ. At low-light levels, the effect of this coupling would be to increase the dark noise σ_D at the rod terminal relative to that measured in the outer segment. This additional noise would increase the midpoint of the optimal nonlinearity defined in Equation 1.

Model 1: Nonlinearity after Pooling

Rod signals were converted to predicted bipolar responses in three steps. (1) Responses of each rod input to the bipolar were summed linearly. (2) The summed signal was passed through a time-independent nonlinearity. (3) Noise was added to represent response fluctuations intrinsic to the bipolar cell.

The first step in the model was to sum the signals from the collection of N rods providing input to the bipolar. We calculated the distribution of the summed signals, $P_{\text{sum}}(A)$, by convolving the distribution of the rod signals given in Equation 3 with itself N times. Next, we applied an instantaneous nonlinear weighting function, $w(A)$. Each amplitude A was multiplied by the corresponding weight $w(A)$ and the distribution of these rescaled amplitudes computed from $P_{\text{sum}}(A)$. Finally, the distribution of weighted signals was convolved with a Gaussian representing noise intrinsic to the bipolar cell; this noise was estimated from sections of record in darkness.

Model 2: Nonlinearity before Pooling

Rod signals were converted to predicted bipolar responses in three steps. (1) Responses of each rod input to the bipolar were passed through a time-independent nonlinearity. (2) The resulting weighted signals were summed linearly. (3) Noise was added to these weighted signals to represent noise intrinsic to the bipolar cell.

The distribution of rod responses from Equation 3 was first weighted by $w(A)$. The distribution of the weighted signals was convolved with itself N times to account for linear summation of the weighted rod inputs. This distribution was convolved with a Gaussian representing noise intrinsic to the bipolar cell.

Acknowledgments

We thank E.J. Chichilnisky and Valerie Uzzell for stimulating discussions; Denis Baylor, E.J. Chichilnisky, Peter Detwiler, and A.P. Sampath for comments on the manuscript; Jim Hurley for providing mice; and Eric Martinson and Maria McKinley for excellent technical assistance. Support was provided to F.R. by the NIH through grant EY-11850 and by the McKnight Foundation.

Received: December 18, 2001

Revised: April 2, 2002

References

- Ashmore, J.E., and Falk, G. (1980). The single-photon signal in rod bipolar cells of the dogfish retina. *J. Physiol. (Lond.)* 300, 151–166.
- Baylor, D.A., Lamb, T.D., and Yau, K.-W. (1979a). The membrane current of single rod outer segments. *J. Physiol. (Lond.)* 288, 589–611.
- Baylor, D.A., Lamb, T.D., and Yau, K.-W. (1979b). Responses of retinal rods to single-photons. *J. Physiol. (Lond.)* 288, 613–634.
- Baylor, D.A., Matthews, G., and Yau, K.-W. (1980). Two components of electrical dark noise in toad retinal rod outer segments. *J. Physiol. (Lond.)* 309, 591–621.
- Baylor, D.A., Nunn, B.J., and Schnapf, J.L. (1984). The photocurrent, noise and spectral sensitivity of rods of the monkey *Macaca fascicularis*. *J. Physiol. (Lond.)* 357, 575–607.
- Belgum, J.H., and Copenhagen, D.R. (1988). Synaptic transfer of rod signals to horizontal and bipolar cells in the retina of the toad (*Bufo marinus*). *J. Physiol. (Lond.)* 396, 225–245.
- Bialek, W., and Owen, W.G. (1990). Temporal filtering in retinal bipolar cells: elements of an optimal computation? *Biophys. J.* 58, 1227–1233.
- Dacheux, R.F., and Raviola, E. (1986). The rod pathway in the rabbit retina: a depolarizing bipolar and amacrine cell. *J. Neurosci.* 6, 331–345.
- DeVries, S.H., and Baylor, D.A. (1995). An alternative pathway for signal flow from rod photoreceptors to ganglion cells in mammalian retina. *Proc. Natl. Acad. Sci. USA* 92, 10658–10662.
- DeVries, H., and Stuijver, M. (1961). The absolute sensitivity of the human sense of smell. In *Principles of Sensory Communication*, W.A. Rosenblith, ed. (Cambridge, MA: MIT Press), pp. 159–167.
- Euler, T., and Masland, R.H. (2000). Light-evoked responses of bipolar cells in a mammalian retina. *J. Neurophysiol.* 83, 1817–1829.
- Hack, I., Peichl, L., and Brandstätter, J.H. (1999). An alternative pathway for rod signals in the rodent retina: rod photoreceptors, cone bipolar cells and the localization of glutamate receptors. *Proc. Natl. Acad. Sci. USA* 96, 14130–14135.
- Hildebrand, J.G., and Shepherd, G.M. (1997). Mechanisms of olfactory discrimination: converging evidence for common principles across phyla. *Annu. Rev. Neurosci.* 20, 595–631.
- Kim, K.J., and Rieke, F. (2001). Temporal contrast adaptation in the input and output signals of salamander retinal ganglion cells. *J. Neurosci.* 21, 287–299.
- Nakatani, K., Tamura, T., and Yau, K.-W. (1991). Light adaptation in retinal rods of the rabbit and two other nonprimate mammals. *J. Gen. Physiol.* 97, 413–435.
- Rao, R., Buchsbaum, G., and Sterling, P. (1994). Rate of quantal transmitter release at the mammalian rod synapse. *Biophys. J.* 67, 57–63.
- Rao-Mirotnik, R., Harkins, A.B., Buchsbaum, G., and Sterling, P. (1995). Mammalian rod terminal: architecture of a binary synapse. *Neuron* 14, 561–569.
- Rieke, F. (2000). Mechanisms of single-photon detection in rod photoreceptors. *Methods Enzymol.* 316, 186–202.
- Rieke, F. (2001). Temporal contrast adaptation in salamander bipolar cells. *J. Neurosci.* 21, 9445–9454.
- Rieke, F., and Schwartz, E.A. (1996a). Asynchronous transmitter release: control of exocytosis and endocytosis at the rod synapse. *J. Physiol. (Lond.)* 493, 1–8.
- Rieke, F., and Baylor, D.A. (1996b). Molecular origin of continuous dark noise in rod photoreceptors. *Biophys. J.* 71, 2553–2572.
- Rieke, F., and Baylor, D.A. (1998). Single-photon detection by rod cells of the retina. *Rev. Mod. Phys.* 70, 1027–1036.
- Robson, J.G., and Frishman, L.J. (1995). Response linearity and kinetics of the cat retina: the bipolar cell component of the dark-adapted electroretinogram. *Vis. Neurosci.* 12, 837–850.

- Schneeweis, D.M., and Schnapf, J.L. (1995). Photovoltage of rods and cones in the macaque retina. *Science* 268, 1053–1056.
- Schneeweis, D.M., and Schnapf, J.L. (2000). Noise and light adaptation in rods of the macaque monkey. *Vis. Neurosci.* 17, 659–666.
- Smith, R.G., Freed, M.A., and Sterling, P. (1986). Microcircuitry of the dark-adapted cat retina: functional architecture of the rod-cone network. *J. Neurosci.* 6, 3505–3517.
- Soucy, E., Wang, Y., Nirenberg, S., Nathans, J., and Meister, M. (1998). A novel signaling pathway from rod photoreceptors to ganglion cells in mammalian retina. *Neuron* 21, 481–493.
- Sterling, P., Freed, M.A., and Smith, R.G. (1988). Architecture of rod and cone circuits to the on-beta ganglion cell. *J. Neurosci.* 8, 623–642.
- Tsukamoto, Y., Morigiwa, K., Ueda, M., and Sterling, P. (2001). Microcircuits for night vision in mouse retina. *J. Neurosci.* 21, 8616–8623.
- van Rossum, M.C., and Smith, R.G. (1998). Noise removal at the rod synapse of mammalian retina. *Vis. Neurosci.* 15, 809–821.
- Walraven, J., Enroth-Cugell, C., Hood, D.C., MacLeod, D.I.A., and Schnapf, J.L. (1990). The control of visual sensitivity. In *Visual Perception: The Neurophysiological Foundations*, L. Spillmann and S.J. Werner, eds. (San Diego: Academic Press) pp. 53–101.
- Werblin, F.S. (1978). Transmission along and between rods in the tiger salamander retina. *J. Physiol. (Lond.)* 280, 449–470.
- Witkovsky, P., Schmitz, Y., Akopian, A., Krizaj, D., and Tranchina, D. (1997). Gain of rod to horizontal cell synaptic transfer: relation to glutamate release and a dihydropyridine-sensitive calcium current. *J. Neurosci.* 17, 7297–7306.
- Wu, S.M. (1987). Synaptic connections among retina neurons in living slices. *J. Neurosci. Methods* 20, 139–149.